Geosci. Model Dev. Discuss., https://doi.org/10.5194/gmd-2017-229
Manuscript under review for journal Geosci. Model Dev.
Discussion started: 11 October 2017
© Author(s) 2017. CC BY 4.0 License.

Geoscientific Model Development Discussions

ARTS, the atmospheric radiative transfer simulator — version 2.2, the planetary toolbox edition

Stefan A. Buehler[1], Jana Mendrok[2], Patrick Eriksson[2], Agnès Perrin[4], Richard Larsson[5], and Oliver Lemke[1]

[1]Meteorologisches Institut, Centrum für Erdsystem- und Nachhaltigkeitsforschung (CEN), Fachbereich Geowissenschaften, Fakultät für Mathematik, Informatik und Naturwissenschaften, Universität Hamburg, Bundesstrasse 55, 20146 Hamburg, Germany
[2]Department of Space, Earth and Environment, Chalmers University of Technology, SE-41296 Gothenburg, Sweden
[4]Laboratoire de Météorologie Dynamique/IPSL, UMR CNRS 8539, Ecole Polytechnique, Université Paris-Saclay, RD36, 91128 PALAISEAU Cedex, France
[5]National Institute of Information and Communications Technology, 4 Chome-2-1 Nukui Kitamachi, Koganei, Tokyo JP-184-0015, Japan

Correspondence to: S. A. Buehler (stefan.buehler@uni-hamburg.de)

Abstract. This article describes the latest stable release (version 2.2) of the Atmospheric Radiative Transfer Simulator (ARTS), a public domain software for radiative transfer simulations in the thermal spectral range (microwave to infrared). The main feature of this release is a planetary toolbox, that allows simulations for the planets Venus, Mars, and Jupiter, in addition to Earth. This required considerable model adaptations, most notably in the area of gaseous absorption calculations. Several other new features are also described, notably radio link budgets, back-scattering radar simulations, and the treatment of Faraday rotation and Zeeman splitting.

1 Introduction

Numerical radiative transfer (RT) modeling with computers perhaps started from the urge to understand atmospheric radiant energy fluxes. The earliest general circulation model (Phillips, 1956) did not yet include a radiation scheme, but simply assumed a globally constant radiative heating rate. In the same year, Plass (1956) already published an article describing numerical simulations of infrared radiation. This paved the way for simple one-dimensional radiative convective models of Earth's energy balance (Manabe and Möller, 1961), and later for global circulation models with sophisticated radiation schemes. It is fair to say that numerical radiative transfer simulations started as soon as computers were becoming available to atmospheric scientists. Since then, the atmospheric sciences have had a constant need for ever more accurate and efficient RT simulation software.

Besides radiative energy flux calculation, the other important application area for RT software is remote sensing. This started almost at the same time as the energy flux simulations, an early example is Kaplan (1959). From the early days on, computer codes for energy flux computation and remote sensing simulations have developed in parallel, but nearly independently, and few codes can be used for both applications. A notable exception is the family of models by AER (Atmospheric and Environmental Research, Clough et al., 2005).

Geosci. Model Dev. Discuss., https://doi.org/10.5194/gmd-2017-229
Manuscript under review for journal Geosci. Model Dev.
Discussion started: 11 October 2017
© Author(s) 2017. CC BY 4.0 License.

Geoscientific Model Development Discussions
Open Access
EGU

A similar partitioning exists even inside the remote sensing RT codes. Historically, most codes were developed for a particular sensor, or remote sensing technique, so that there are dedicated codes for active or passive sensors, microwave, infrared, or ultraviolet/visible frequencies, and up-looking, down-looking, or limb-looking geometry. Moreover, such partitioning also exists regarding the object of observation like the different bodies of the solar system.

Radiative transfer models for planets other than Earth have been developed about equally as long as such for Earth itself (e.g., Cess, 1971). Also, terrestrial radiative transfer codes have frequently been used to simulate spectra of solar system as well as exo-planets with certain modifications or extensions of, e.g., the spectroscopic data applied (e.g. Urban et al., 2005; Bernstein et al., 2007; Kasai et al., 2012; Vasquez et al., 2013; Schreier et al., 2014). Few have been explicitly developed with a view on applicability to a wide range of planet characteristics, i.e. to be able to treat very different basic composition of the atmospheres, wide ranges of atmospheric temperatures, etc., like e.g. VSTAR (Versatile Software for Transfer of Atmospheric Radiation, Bailey and Kedziora-Chudczer, 2012). Interest in prediction and analysis of non-Earth spectra has increased significantly in recent years in relation with intensified research into habitability of planets and the search for exoplanets, calling also for more consistent and more generally applicable models.

Regarding Earth observations, the separate development of models for spectral regions or measurement techniques now proves to be an obstacle for synergistic use of modern multi-sensor observations, which requires consistency in the simulation of all involved sensors. Out of an appreciation of this, a few RT codes have been developed that are fairly broad in scope, agnostic of a particular sensor, and used for a wide range of applications. Besides the already mentioned AER model family, libRadtran (Emde et al., 2016) could be named here as a multi-purpose model toolbox for the visible and infrared spectral range, as well as Dudhia (2017) and Schreier et al. (2014) as general-purpose models for the infrared spectral range; and of course the Atmospheric Radiative Transfer Simulator (ARTS), the subject of this article.

The ARTS project started in the year 2000 as a joint initiative of Patrick Eriksson (Chalmers) and Stefan Buehler (then at University of Bremen). Right from the start the code was open source (GNU's Not Unix (GNU) public license); the current version is freely available at www.radiativetransfer.org. At the start, the model focused on simulating clear-sky limb observations of Earth's atmosphere in the millimeter and sub-millimeter spectral range, because that was the main interest of the authors (Eriksson et al., 2002; Buehler et al., 2005b). Pretty soon, the interests widened, and ARTS adopted new capabilities such as simulating downlooking meteorological microwave sensors (Buehler et al., 2004; John and Buehler, 2004) and active radio link measurements (Eriksson et al., 2003). ARTS was also started to be used for infrared energy flux simulations (Buehler et al., 2006b; John et al., 2006), and the capability to handle cases with scattering by hydrometeors was developed by two different scattering solvers, the discrete ordinate iterative solver (DOIT, Emde et al., 2004a, b), employed for example in Rydberg et al. (2007) and Sreerekha et al. (2008), and a Monte Carlo solver (MC, Davis et al., 2005, 2007), for example used in Rydberg et al. (2009) and Eriksson et al. (2011d).

Over the years, the model was validated by several inter-comparison studies for example by Melsheimer et al. (2005) and Buehler et al. (2006a). Most recently, the ARTS infrared energy flux calculations were used as one of the reference models in a broad assessment of the quality of radiation codes in climate models (Pincus et al., 2015), and were shown to be in very good agreement with the other participating reference models. Also, closure studies with radiosondes, microwave observations, and

Geosci. Model Dev. Discuss., https://doi.org/10.5194/gmd-2017-229
Manuscript under review for journal Geosci. Model Dev.
Discussion started: 11 October 2017
© Author(s) 2017. CC BY 4.0 License.

infrared observations increase our confidence that the model consistently handles the different spectral ranges (Kottayil et al., 2012).

Perhaps the most significant limitation, though, that remains even to date, is that ARTS does not have a collimated beam source, so it currently cannot simulate solar radiation observations or solar radiation energy fluxes. The line-by-line absorption calculation itself, however, does work also in the solar spectral range, and has been used by Gasteiger et al. (2014) to precalculate absorption cross sections for libRadtran (Emde et al., 2016), using the simulated annealing method described in (Buehler et al., 2010).

There are only two previous publications that describe earlier versions of ARTS as a whole, Buehler et al. (2005a) and Eriksson et al. (2011a), but many of the main building blocks of ARTS and the tools around it have been described in dedicated publications. Besides the already mentioned DOIT and MC scattering solvers, important building blocks are the method to pre-calculate and store gas absorption data (Buehler et al., 2011) and the method to handle sensor characteristics by building up a comprehensive sparse matrix sensor representation (Eriksson et al., 2006).

Important tools around ARTS are the Qpack Matlab package (Eriksson et al., 2005) that, among many other things, allows optimal estimation inversions (going from measured or simulated radiation back to an estimate of the atmospheric state), and a Matlab package for frequency grid optimisation by simulated annealing (Buehler et al., 2010), which both are part of the bigger Matlab package ATMLAB (ATMospheric matLAB), freely available from the ARTS website. The website also holds arts-xml-data, a data package with model atmospheres, spectroscopic data, and other data that are required or useful for running radiative transfer simulations. And, last but not least, there is a growing set of Python interface and helper functions, collected in a package called Typhon.

This article describes ARTS version 2.2. The most visible difference to prior versions is that the program, originally developed for Earth, has been adapted to also work well for the other solar system planets, specifically Mars, Venus, and Jupiter. These additions were developed in a study supported by the European Space Agency (ESA). Along with the program itself comes a set of inputs for the different planets, such as spectroscopic parameters, atmospheric composition, and basic parameter settings such as the planet's radius. Together, program and input data form what we call the planetary toolbox. Details on the input data and the actual performance of the model relative to planetary observations will be the subject of another planned article.

Besides the planetary toolbox, there were numerous other additions and improvements: To start with, ARTS now includes collision induced absorption continua from the HIgh-resolution TRANsmission molecular absorption database (HITRAN, Richard et al., 2012). This addition was triggered by the urgent need for some of these continua for other planets, but they may be useful for Earth as well.

Another change is, that the program generally has far fewer internal constants now, which instead are read from input files; or that rather can be read, because there are still built-in default values for convenience. This applies for example to isotopologue ratios and to spectroscopic partition functions. Also in the area of spectroscopy, pressure broadening has been generalised to use separate broadening parameters for all major broadening gas species of the different planets.

Geosci. Model Dev. Discuss., https://doi.org/10.5194/gmd-2017-229
Manuscript under review for journal Geosci. Model Dev.
Discussion started: 11 October 2017
© Author(s) 2017. CC BY 4.0 License.

Geoscientific Model Development Discussions

Capabilities to simulate active observations have been enhanced by handling simple radar backscattering (without multiple scattering), and by correctly treating Faraday rotation for radio links. The Faraday rotation uses a Stokes vector formalism where the extinction term in the scalar radiative transfer equation is replaced by a four-by-four propagation matrix.

The Stokes formalism for Faraday rotation has benefited greatly from the experience gathered with the last important addition that has to be mentioned here: the capability to simulate Zeeman splitting in a physically rigorous way, which is also handled by a Stokes vector formalism, described in Larsson et al. (2014); Larsson (2014). The method has been validated against observations in uplooking (Navas-Guzmán et al., 2015) and downlooking (Larsson et al., 2016) geometry, and also has already been employed for some sensitivity and retrieval simulation studies (Larsson et al., 2013, 2017).

The main purpose of this article is to introduce, explain, and document these recent extensions and modifications, and to serve as a reference for this version of ARTS. The structure is as follows: Section 2 describes the planetary toolbox extensions and modifications, Section 3 describes other modifications and extensions, and Section 4 contains summary and outlook.

2 From Earth to planets: generalized propagation modeling methods

When extending radiative transfer modelling from Earth to other planets, the major challenge is to remove a number of assumptions on basic physical parameters made in the model itself or in the input data. This includes hard-coding of constants that are valid (and constant), for Earth but might differ between planets. It furthermore regards assumptions in certain algorithms and parametrisations. The most prominent one is the expression of spectroscopic parameters of gas absorption lines like foreign pressure broadening and pressure induced frequency shifts by a single parameter valid for the standard mixture of air (79% N_2+21% O_2). Here, the limitation is not only in the RT model itself, but spectroscopic catalogues commonly report the Earth-valid, standard air parameters only.

ARTS has been revised for such assumptions, and modifications towards more general approaches have been made. Below we detail the most relevant of them.

2.1 Line spectroscopy

Spectral lines are broadened by collision of gas molecules with other gas molecules. The line width then scales with the partial pressure of the perturbing species. The constant of proportionality is specific to each transition and to the species involved.

Commonly in line-by-line absorption modeling, self broadening and foreign or air broadening are distinguished. The total line width is the sum of the self broadened line width and the foreign broadened line width. The self broadened line width scales with the partial pressure of the species itself, while the foreign broadened line width scales with the total pressure minus the partial pressure of the species itself. (For an explicit mathematical formulation, see Equation 1 further down.) It is typically the respective broadening proportionality constants, or broadening coefficients, of self and foreign broadening, which are reported in the spectral line catalogues.

For line catalogues focusing on Earth applications, the reported foreign broadening coefficient is derived for a standard air mixture of 79% N_2 and 21% O_2. When considering other planets than Earth, the assumption of air as a nitrogen-oxygen-

Geosci. Model Dev. Discuss., https://doi.org/10.5194/gmd-2017-229
Manuscript under review for journal Geosci. Model Dev.
Discussion started: 11 October 2017
© Author(s) 2017. CC BY 4.0 License.

Geoscientific Model Development Discussions

mixture does not hold anymore. Instead, the composition of the atmosphere largely varies from planet to planet. Since pressure broadening is specific to the species involved, atmospheric composition affects the pressure broadening. Hence, for exact calculations the true composition needs to be considered.

In principle, this can be and often is handled in the way that the concept of a foreign broadening coefficient given for a standard air mixture is kept. This requires the compilation of spectral line catalogues specific to the atmospheric composition in question, i.e., the compilation of catalogues specific to individual planets. A more flexible option, though, is to explicitly report broadening parameters for the variety of broadening gases in the line catalogue and derive the foreign broadening coefficient from them just-in-time considering the actual atmospheric composition. The latter approach has been chosen for ARTS.

In addition to the line broadening, gas molecule collisions cause pressure dependent frequency shifts of the transitions, also called pressure shifts. Just as the broadening, the pressure shifts are specific to each transition and the species involved in the collision. Commonly, only an overall pressure shift parameter is reported in line catalogues and applied in the line-by-line absorption modeling. Regarding applicability in atmospheres of different compositions, similar considerations as presented for line broadening apply to pressure shifts.

Earlier ARTS versions (Buehler et al., 2005a; Eriksson et al., 2011a) follow the common approach of standard air foreign broadening and pressure shift parameters, calculating the pressure broadened line width γ_L as

$$\gamma_L = x_\mathrm{s}\, p\, \gamma_\mathrm{s} \left(\frac{T_\mathrm{ref}}{T}\right)^{n_\mathrm{s}} + (1 - x_\mathrm{s})\, p\, \gamma_\mathrm{a} \left(\frac{T_\mathrm{ref}}{T}\right)^{n_\mathrm{a}}, \tag{1}$$

where the first term on right hand side denotes the self broadening width $\gamma_{L\mathrm{s}}$ and the second one the foreign or air broadening width $\gamma_{L\mathrm{a}}$. In Equation 1, γ_s and γ_a are the self and the air broadening parameters, n_s and n_a are the temperature exponents for γ_s and γ_a, respectively, and T_ref is the reference temperature of the broadening parameters. All these parameters are reported in spectroscopic catalogues (the reference temperature often only implicitly for the entire catalogue). Furthermore, x_s is the volume mixing ratio (VMR) of the transition species, p is the total atmospheric pressure and T is the atmospheric temperature. The pressure shift $\Delta\nu$ is calculated as

$$\Delta\nu = p\, \delta\nu \left(\frac{T_\mathrm{ref}}{T}\right)^{(0.25+1.5*n_\mathrm{air})}, \tag{2}$$

where $\delta\nu$ is the pressure shift parameter reported in spectroscopic catalogues. Note that to our knowledge there is no generally accepted formulation for the temperature dependence of $\Delta\nu$ and that Equation 2 simply reports the expression applied in ARTS, without any claim of general validity.

To allow for flexible air compositions, the foreign broadening width $\gamma_{L\mathrm{a}}$ has been reformulated into a weighted sum of the broadening contributions from individual broadening species as

$$\gamma_{L\mathrm{a}} = (1 - x_\mathrm{s})\, p\, \frac{\sum_i \left[x_i\, \gamma_i\, \left(\frac{T_\mathrm{ref}}{T}\right)^{\mathrm{n}_i}\right]}{\sum_i x_i}, \tag{3}$$

Geosci. Model Dev. Discuss., https://doi.org/10.5194/gmd-2017-229
Manuscript under review for journal Geosci. Model Dev.
Discussion started: 11 October 2017
© Author(s) 2017. CC BY 4.0 License.

Geoscientific Model Development Discussions
Open Access
EGU

where γ_i is the broadening parameter of the i^{th} broadening species, n_i its temperature coefficient, and x_i the VMR of the broadening species. Accordingly, pressure shift $\Delta\nu$ is rewritten as

$$\Delta\nu = p \frac{\sum_i \left[x_i \, \delta\nu_i \, \left(\frac{T_{\text{ref}}}{T}\right)^{(0.25+1.5*\text{n}_i)} \right]}{\sum_i x_i} \,, \tag{4}$$

with $\delta\nu_i$ being the pressure shift due to the i^{th} broadening, or rather shifting, species. Note that, like Equation 2, Equation 4 simply states the formula used in ARTS, without claiming general validity.

Commonly, the atmospheric composition is not specified in such detail that the sum over the VMR of all considered species adds up to 1. For the classical approach, Equations 1 and 2, this does not matter as the contribution from all foreign gases is taken into account by weighting the foreign contribution with the total foreign air pressure ($(1 - x_{\text{s}})\, p$). For the revised approach, Equations 3 and 4, the normalisation by $\sum_i x_i$ balances out deviations from a VMR sum of 1.

A completely general approach would have to take into account γ_i and n_i for all possible atmospheric gas species i. Since contributions of individual species scale with their VMR, it is sufficient to cover the major atmospheric gas species and neglect minor trace gas species. Currently, ARTS 2.2 considers N_2, O_2, H_2O, CO_2, H_2, and He as foreign broadening species. This selection covers the most abundant species in the atmospheres of Earth, Venus, Mars, and Jupiter, the planets the toolbox has been developed for. The approach itself is generally applicable, and the ARTS implementation could easily be modified to cover further foreign species.

Note, that this new broadening mechanism has advantages even for Earth's atmosphere. To give an example, the broadening of oxygen lines by water vapor is quite different from their nitrogen broadening, and complete absorption models such as that of Rosenkranz (1993) take into account this effect, which makes oxygen lines broader in a very wet atmosphere. So far, it was not possible to treat this effect with a generic line-by-line calculation based on an external catalog, but with the species-specific broadening parameters in the new ARTS catalogue it happens automatically, if parameters for the broadening by water vapor are available.

To use the new mechanism in practice, broadening and shift parameters for all broadening gases have to be provided by a line catalogue. We have compiled such a catalogue. Details of the compilation are presented in Section 2.2 below.

It should be noted that both the classical and the revised broadening and shift calculation approach are available with ARTS 2.2 and will be kept in future versions. The approach applied in the actual calculation is governed by the format of the spectral line data provided (for further details see Section 2.2) and requires no specific settings by the user. Since data formats for different line transitions are allowed to differ, it is possible to apply both line calculation approaches within one model run. Having both mechanisms available also simplified the testing of the new and more complex treatment, in order to ensure that the results are consistent with the old treatment where they should be.

2.2 Line catalogue

ARTS has its own internal representation of spectral line data that maps naturally to a native catalogue format. Two variants of this internal catalogue data exist, corresponding to the two line broadening and shift algorithms introduced above.

Geosci. Model Dev. Discuss., https://doi.org/10.5194/gmd-2017-229
Manuscript under review for journal Geosci. Model Dev.
Discussion started: 11 October 2017
© Author(s) 2017. CC BY 4.0 License.

Geoscientific Model Development Discussions

Beside other spectroscopic parameters, the catalogue format related to the classical algorithm, called ARTSCAT-3, contains the air broadening and shift parameters γ_a, n_a, and $\delta\nu$ representative for Earth conditions. Besides its internal formats, ARTS can digest other catalogues with different formats, e.g. the HITRAN format. These other databases typically report "classical" Earth representative spectroscopic parameters, hence their data are internally converted to ARTSCAT-3 format. A detailed description of the ARTSCAT-3 format is given in Eriksson et al. (2011b).

The ARTS internal catalogue format corresponding to the revised line broadening and shift algorithm, called ARTSCAT-4, reports broadening and shift parameter for individual foreign species. As already stated above, the currently covered broadening species are the most abundant species in the atmospheres of Earth, Venus, Mars, and Jupiter, namely N_2, O_2, H_2O, CO_2, H_2, and He. The complete format definition is given in Table 1.

As part of the planetary toolbox, spectroscopic data have been compiled and made available with the arts-xml-data package. This is not the first effort to create a dedicated spectroscopic line list for ARTS: already in 2005, an ESA funded study lead to a dedicated line list for millimeter/sub-millimeter limb sounding instruments (Perrin et al., 2005; Verdes et al., 2005). However, the old line list covered only selected bands, whereas the new line list covers a much broader spectral range.

In line with the scope of the planetary toolbox, to provide tools and data for propagation modeling in the atmospheres of Venus, Mars, and Jupiter as well as Earth in the spectral domain up to 3 THz, the line catalogue has been generated for gaseous absorption species considered of interest in these planets' atmospheres and for the range of atmospheric conditions of these planets. An overview of the species considered is given in Table 2.

The foreign species specific spectroscopic line parameters have been compiled from literature or extracted from the HITRAN (HIgh-resolution TRANsmission molecular absorption database, Rothman et al., 2009, 2013), GEISA (Gestion et Etude des Informations Spectroscopiques Atmosphériques, Jacquinet-Husson et al., 2011), and JPL (Jet Propulsion Laboratory, Pickett et al., 1998) spectroscopic databases. The sources of the data are given explicitly and in detail for each molecule in Mendrok et al. (2014). Selected examples of the compilation procedure are detailed below. Species of obvious planetological interest but without line absorption signatures in the THz region, like ethane, germane, ethylene, or benzine, have been neglected.

In order to be able to also use the database for Earth applications, species only relevant in the Earth atmosphere, but none of the other planets (see Table 2) have been included as well. Line parameters of these species have been taken from the HITRAN edition current at the time of compilation (Rothman et al., 2013, update 13.06.2013) and converted to ARTSCAT-3 format without any further changes. Note that using ARTS functionality, users themselves can create ARTSCAT spectroscopic files from HITRAN data, e.g. from more recent editions or updates.

When compiling the foreign species specific line parameters, explicit values have been put where available. These have been derived by a careful literature investigation searching for experimental or theoretical studies specifically devoted to line broadening and shift by He, H_2, CO_2, or H_2. Furthermore, air broadening and shift parameters reported in the HITRAN database are often deduced from individually determined and reported N_2 and O_2 broadening and shift data. In such cases, we applied the original N_2 and O_2 literature data in our catalogue compilation. However, for a given species, absorption line and perturbing gas, the broadening and line shift parameters are often absent in the literature, simply because spectroscopic studies

Geosci. Model Dev. Discuss., https://doi.org/10.5194/gmd-2017-229
Manuscript under review for journal Geosci. Model Dev.
Discussion started: 11 October 2017
© Author(s) 2017. CC BY 4.0 License.

Geoscientific Model Development Discussions
Open Access
EGU

Table 1. ARTSCAT-4 spectroscopic line data format. Column #0 gives the line entry start marker, the following parameters are separated by one or more blanks.

Column	Parameter	Symbol	Unit
0	'@'	-	-
1	molecule & isotopologue tag	-	-
2	center frequency	ν_0	Hz
3	line intensity	S_0	Hz m^2
4	reference temperature	T_{ref}	K
5	lower state energy	E_{l}	J
6	Einstein A-coefficient	A	1/s
7	Upper state stat. weight	g_{u}	-
8	Lower state stat. weight	g_{l}	-
9	broadening parameter self	γ_{s}	Hz/Pa
10	broadening parameter N2	γ_{N2}	Hz/Pa
11	broadening parameter O2	γ_{O2}	Hz/Pa
12	broadening parameter H2O	γ_{H2O}	Hz/Pa
13	broadening parameter CO2	γ_{CO2}	Hz/Pa
14	broadening parameter H2	γ_{H2}	Hz/Pa
15	broadening parameter He	γ_{He}	Hz/Pa
16	broadening temp. exponent self	n_{s}	-
17	broadening temp. exponent N2	n_{N2}	-
18	broadening temp. exponent O2	n_{O2}	-
19	broadening temp. exponent H2O	n_{H2O}	-
20	broadening temp. exponent CO2	n_{CO2}	-
21	broadening temp. exponent H2	n_{H2}	-
22	broadening temp. exponent He	n_{He}	-
23	frequency pressure shift N2	$\delta\nu_{\mathrm{N2}}$	Hz/Pa
24	frequency pressure shift O2	$\delta\nu_{\mathrm{O2}}$	Hz/Pa
25	frequency pressure shift H2O	$\delta\nu_{\mathrm{H2O}}$	Hz/Pa
26	frequency pressure shift CO2	$\delta\nu_{\mathrm{CO2}}$	Hz/Pa
27	frequency pressure shift H2	$\delta\nu_{\mathrm{H2}}$	Hz/Pa
28	frequency pressure shift He	$\delta\nu_{\mathrm{He}}$	Hz/Pa
29	quantum number information	-	-

dealing with these line parameters were never performed. In this case, the values quoted in our catalogue have been reasonably estimated, where the estimation strategy could differ from one absorption species to the other.

Geosci. Model Dev. Discuss., https://doi.org/10.5194/gmd-2017-229
Manuscript under review for journal Geosci. Model Dev.
Discussion started: 11 October 2017
© Author(s) 2017. CC BY 4.0 License.

Geoscientific Model Development Discussions
Open Access
EGU

Table 2. Overview of the absorption species covered by the ARTS spectroscopic database. For "planet interest" species, ARTSCAT-4 type data with foreign species specific line parameters has been compiled, while data for "Earth-only" species has been taken from HITRAN without modifications and is provided in ARTSCAT-3 format. Empty data files are provided for "no transition" species, which exhibit no absorption lines within the spectral region of interest of the planetary toolbox, but have to be considered as perturbing species. Species with "ARTS 2.0" history are known species in ARTS' pre-toolbox version. "New" species have been added in ARTS 2.2 with species data taken from HITRAN (default) or other sources like the JPL database (denoted by '*').

species group	history	species
planet interest	ARTS 2.0	H_2O, CO_2, O_3, CO, CH_4, O_2, SO_2, NH_3, HF, HCl, OCS, H_2CO, H_2O_2, PH_3, H_2S, HO_2, H_2SO_4
	new	SO*, C_3H_8*
Earth-only	ARTS 2.0	N_2O, NO, NO_2, HNO_3, OH, HBr, HI, ClO, HOCl, HCN, CH_3Cl, HCOOH, O, HOBr
	new	CH_3OH
no THz transition	ARTS 2.0	N_2
	new	H_2, He*

In particular, for the line broadening parameters, the values have been estimated from those existing in the literature for similar molecules or transitions. For water vapor, for example, numerous experimental and theoretical studies deal with its pressure broadening by CO_2 (Gamache et al., 2011, and references therein). Comparing the air and CO_2 broadening parameters we estimate them being related by $\gamma_{\mathrm{CO2}} \sim 1.55\gamma_{\mathrm{a}}$, and we used this expression in our catalogue compilation to derive γ_{CO2} anytime it is otherwise unknown. Similarly, for water vapor transitions we estimated from the existing literature values $\gamma_{\mathrm{N2}} \sim 1.1016\gamma_{\mathrm{a}}$, $\gamma_{\mathrm{O2}} \sim 0.6178\gamma_{\mathrm{a}}$, and $\gamma_{\mathrm{He}} \sim 0.24\gamma_{\mathrm{a}}$. For ozone, $\gamma_{\mathrm{N2}} \sim 1.029\gamma_{\mathrm{a}}$ and $\gamma_{\mathrm{O2}} \sim 0.89\gamma_{\mathrm{a}}$ were deduced from the literature. We applied these relations to derive the respective γ_i from γ_{a} quoted in HITRAN for all water and ozone lines for which this information is otherwise missing. For ozone and other molecules, for which no γ_{He} data exist in the literature, a default relation of $\gamma_{\mathrm{He}} = 0.25\gamma_{\mathrm{a}}$ was used to estimate γ_{He}. Regarding γ_{N2} and γ_{O2}, we carefully checked that their values are consistent with their HITRAN γ_{a} counterpart, i.e. to fulfill the condition $\gamma_a = 0.79\gamma_{\mathrm{N2}} + 0.21\gamma_{\mathrm{O2}}$ whenever this scaling strategy was applied.

For several linear molecules, like CO, HCl, HF and CO_2, a polynomial dependence of the N_2, O_2 and CO_2 broadening parameters to the rotational quantum numbers m was established from measurements reported in the literature (Le Moal and Severin, 1986; Varanasi, 1975). For our compilation, we derived the γ_{N2}, γ_{O2}, and γ_{CO2} using these expressions.

For some other molecules, e.g. SO_2, very precise line broadening parameters exist in the literature, however only for a very restricted set of rotational transitions when compared to the full list of lines in the spectral region up to 3 THz. Clearly, it is not possible to estimate the rotational dependence of these broadening parameters from these limited data. In these cases, the mean values deduced from the experimental data were implemented in our catalogue compilation.

For cases when the pressure broadening parameter of a perturber is not known at all, the default value adopted in HITRAN ($\gamma_i = 0.1\,\mathrm{cm}^{-1}$/atm corresponding to $\gamma_i = 30000\,$Hz/Pa in terms of SI units as applied in ARTS) was used. Similarly, the

Geosci. Model Dev. Discuss., https://doi.org/10.5194/gmd-2017-229
Manuscript under review for journal Geosci. Model Dev.
Discussion started: 11 October 2017
© Author(s) 2017. CC BY 4.0 License.

Geoscientific Model Development Discussions

default value $n_i = 0.75$ was set for the pressure broadening temperature exponent. One exception here is helium, for which the default value was estimated as $\gamma_{\mathrm{He}} = 0.04\,\mathrm{cm}^{-1}/\mathrm{atm}$ (12000 Hz/Pa). The pressure shift parameter $\delta\nu$, which is often unknown in the THz region for most of the perturbing gases considered here, has been set to a default value of zero in the absence of any data in the literature.

As indicated above, the primary source for perturber independent parameters like line positions and intensities has been the HITRAN and GEISA databases. However, several molecules considered of interest in planetary atmospheres, specifically in the atmospheres of the three terrestrial planets we focused on here, are so far not covered by HITRAN or GEISA. This concerns for example sulfur monoxide (SO), sulfuric acid (H_2SO_4), propane (C_3H_8) and phosphine (PH_3). To generate the linelists for our catalogue, we used the line positions and intensities quoted in the JPL catalog. The line shape parameters were implemented using the same procedure as described above.

It should be noted that the applied strategy — prefering explicit per-species broadening and shift parameters over deriving them from HITRAN γ_{a} as well as occassional application of parameterisations in terms of quantum numbers — can lead to differences in Earth atmospheric absorption cross sections when calculated from the toolbox catalogue compared to purely HITRAN-based calculations.

Along with the toolbox development, ARTS' list of known absorption species has been revised. It was updated with data from the recent HITRAN (Rothman et al., 2009, 2013) and TIPS (Total Internal Partition Sums, Fischer et al., 2003; Laraia et al., 2011) editions, which introduced a number of new species and isotopologues. Some further species not (yet) in HITRAN, but required for the planetary toolbox, have been added with species data (molecular mass, isotopologue ratio, partition function information) taken from the JPL spectroscopic database (Pickett et al., 1998, retrieved from http://spec.jpl.nasa.gov/) or from educated guesses. The latter regards species that were rated as being of interest in the atmospheres of the toolbox planets and for which spectroscopic line data have been collected (e.g., C_3H_8), but also inert species that are required for the planet-suitable line broadening and shift algorithm introduced (e.g., He). Newly added species are identified in Table 2.

The spectroscopic catalogue data are available from the arts-xml-data package, where data are organised into one file per absorption species. It should be noted that our spectroscopic catalogue is a snapshot in time of the available spectroscopic data of interest for planetary atmospheric remote sensing, at the time of development. The snapshot is as of early 2012, when the catalogue was compiled.

HITRAN, the most commonly used general spectroscopic line database has been undergoing very significant development in recent years (Hill et al., 2013). The new 2016 edition for the first time includes explicit broadening parameters for H_2, He, and CO_2 (Gordon et al., 2017), as well as many other new crucial parameters, for example for handling line mixing. We enthusiastically welcome the new HITRAN paradigm, since it means that it will be possible to drive the new broadening calculation in ARTS with parameters directly from HITRAN in the future. The ARTS interface to the new HITRAN is not yet available, but will be worked on with high priority.

Geosci. Model Dev. Discuss., https://doi.org/10.5194/gmd-2017-229
Manuscript under review for journal Geosci. Model Dev.
Discussion started: 11 October 2017
© Author(s) 2017. CC BY 4.0 License.

Geoscientific Model Development Discussions

2.3 Refractivity

Changes in propagation speed of electromagnetic radiation, described by the refractive index $n = c/\nu_\mathrm{p}$ or the refractivity $N = n - 1$, where ν_p and c are the propagation speed in a medium and in vacuum, respectively, lead to bending of the propagation path of radiation, also called refraction. Neutral gases as well as free electrons contribute to refraction in planetary atmospheres.

Assuming that the refractivity of a gas is proportional to its density (e.g. Newell and Baird, 1965; Stratton, 1968), it can be determined from the refractivity at reference conditions (pressure p_ref and temperature T_ref) and applying a gas law to scale it to other conditions. For a gas mixture, the total refractivity can then be determined as the sum of all partial refractivities, i.e.

$$N = N_{\mathrm{ref},1}\frac{n_1}{n_{\mathrm{ref},1}} + N_{\mathrm{ref},2}\frac{n_2}{n_{\mathrm{ref},2}} + \cdots \tag{5}$$

where N is the total refractivity, $N_{\mathrm{ref},i}$ is the partial refractivity for gas i at reference conditions, n_i is the partial density, and $n_{\mathrm{ref,i}}$ is the reference density. For Earth atmosphere, commonly empirical parametrizations are applied that summarise the air, or at least its dry part, into one component scaled by the total pressure. Water vapor is often considered as a separate component due to its different reference refractivity and its strong variability in abundance (e.g., Thayer, 1974; Mathar, 2007). With $N_{\mathrm{ref},i}$ being specific to the gas species and varying notably between different species, it is obvious that further refined or generalized models are necessary when atmospheric composition is fundamentally different from Earth.

In ARTS 2.2, we have implemented the approach outlined in Equation 5 with species i being individual atmospheric gas species. Reference refractivities of N_2, O_2, CO_2, H_2, and He, derived at 47.7 GHz and considered to be valid for microwave and sumbillimeter-wave frequencies, have been taken from Newell and Baird (1965). To achieve a better agreement with parametrisations for Earth, H_2O is considered, too, and its reference refractivity has been estimated from the parametrisation by Thayer (1974). For scaling to non-reference conditions, we apply the ideal gas law yielding

$$N = \frac{T_\mathrm{ref}}{p_\mathrm{ref}}\sum_{i=1}^{m} N_{\mathrm{ref},i}\frac{p_i}{T} \tag{6}$$

where p_i is the actual partial pressure of species i and T the actual temperature. To account for missing contributions of unconsidered species, the refractivity derived from Equation 6 is normalized to a total volume mixing ratio of 1, similar to the line broadening normalisation in absorption calculations (see Section 2.1). ARTS offers further models specifically for Earth air refractive indices for the microwave (Thayer, 1974) and the infrared spectral region.

Electron contributions are negligible for passive observation techniques, but play a recognizable role for some active techniques like radio links and Global Navigation Satellite System (GNSS) measurements. Neglecting influences of any magnetic field, the refractive index of a plasma like the ionosphere is (e.g., Rybicki and Lightman, 1979)

$$n = \sqrt{1 - \frac{N_\mathrm{e}e^2}{\epsilon_0 m\omega^2}}, \tag{7}$$

Geosci. Model Dev. Discuss., https://doi.org/10.5194/gmd-2017-229
Manuscript under review for journal Geosci. Model Dev.
Discussion started: 11 October 2017
© Author(s) 2017. CC BY 4.0 License.

Geoscientific Model Development Discussions

where ω is the angular frequency ($\omega = 2\pi\nu$), N_e the electron density, e and m the charge and the mass of an electron, respectively, and ϵ_0 the permittivity of free space. This refractive index, which is less than unity but approaching unity with increasing frequency, describes the phase velocity of the radiation, hence determines the ray path. The propagation speed of the signal energy through the plasma, which determines signal delays along the path, is described by the group velocity and the corresponding group refractive index (Rybicki and Lightman, 1979)

$$n_\mathrm{g} = \left(1 - \frac{N_\mathrm{e} e^2}{\epsilon_0 m \omega^2}\right)^{-1/2} = \frac{1}{n}. \tag{8}$$

Electron contribution to the phase and the group velocity index of refraction according to Equations 7 and 8 has been implemented in ARTS 2.2.

2.4 Isotopologue abundances

Absorption coefficients are proportional to the amount of the absorption species and the transition line strength. For practical reasons, the amount is often provided in terms of the volume mixing ratio (VMR) of the species covering all isotopologues, e.g. water vapor VMR instead of the VMR of specific isotopologues like $H_2{}^{16}O$ or HDO. Then, scaling by the relative abundance of the isotopologue is required. The scaling can either be applied to the VMR or the line strength. HITRAN implements the latter approach by providing pre-scaled line strenghts valid for mean Earth conditions. However, as isotopologue abundances differ between planets, this approach is inflexible and inconvenient for planetary applications. ARTS on the other hand applies the VMR scaling approach requiring isotopologue abundance independent line strengths.

For being able to apply HITRAN spectroscopic data, ARTS contains a hard-coded table of relative isotopologue abundances in Earth atmosphere, where the relative abundance is the ratio of abundance of an isotopologue to the abundance of the gas species over all its isotopologues (in contrast, isotopologue ratio refers to the abundance ratio of an isotopologue to the abundance of the main isotopologue of the species; equivalent definitions apply for isotopes). This table is used to convert HITRAN isotopologue scaled line strenghts into ARTS' abundance independent line strengths. In previous ARTS versions, the table was also applied in the VMR scaling of absorption coefficients. In ARTS 2.2, isotopologue abundance has been introduced as a user-accessible variable, which can be initialized from the built-in isotopologue table, e.g. for Earth atmosphere calculations, or read from file, e.g. for planetary use.

As part of the planetary toolbox, tables of relative isotopologue abundances for Venus, Mars, and Jupiter are provided with the arts-xml-data package. Typically, isotopic composition of atmospheres is reported, commonly in terms of isotope ratios, from which isotopologue abundances of molecular species can be derived. The tables provided here have been derived by rescaling Earth isotopologue abundances with planetary isotope ratios retrieved from literature. Isotope ratios of D (in all planets) and ^{15}N (in Mars and Jupiter) were found to significantly differ from Earth values, while other species are within 5% of Earth's values. Adaptation of isotopologue abundances was, hence, restricted to species containing hydrogen and nitrogen. Isotopic ratios applied in the adaptation are reported in Table 3. Earth values were derived from ARTS built-in isotopologue abundances separately per molecular species, hence only an approximate value is given in the table.

Geosci. Model Dev. Discuss., https://doi.org/10.5194/gmd-2017-229
Manuscript under review for journal Geosci. Model Dev.
Discussion started: 11 October 2017
© Author(s) 2017. CC BY 4.0 License.

Geoscientific Model Development Discussions

Table 3. Planetary isotopic ratios as applied in the isotopologue ratio conversion. Earth values are given for reference only, while species specific values were applied in the conversion (see text). Values for Venus, Earth and Mars taken from Lammer et al. (2008, Table 1), Jupiter from Owen and Encrenaz (2003).

Planet	D/H	$^{15}N/^{14}N$
Venus	1.9e-2	as Earth
Earth	(∼1.5e-4)	(∼3.7e-3)
Mars	8.1e-4	5.7e-3
Jupiter	2.6e-5	2.25e-3

2.5 Further adaptations for planetary use

A couple of further planet dependent parameters have been turned into user-controlable parameters. This includes size and shape parameters of ellipsoidal planets, required for line of sight calculations, where also predefined settings for the toolbox planets in the form of dedicated workspace methods are available. This furthermore concerns settings of the gravitational constant and of the molar mass of dry air, both required for deriving altitude-pressure relations assuming hydrostatic equilibrium, as well as the sideareal rotation period of a planet, required for considering Doppler shifts resulting from the rotation of a planet observed from a platform not in orbit around this planet.

3 Further new model features and remaining restrictions

Besides the adaptations described above, which were necessary to make the propagation model applicable to general planetary atmospheres, several other new modeling features are available with the new ARTS version. A major extension is the coverage of additional measurement techniques, specifically of active techniques like radio occultation measurements and radio link budget estimations (Section 3.1), but also backscattering radar observations (Section 3.2). The first ones are of particular interest for the planetary toolbox since they have been suggested or applied for planetary exploration (e.g. Eshleman et al., 1987; Hinson et al., 1997; Oschlisniok et al., 2012). Several physical processes affect both passive and active measurements. Propagation models applying identical algorithms to model these processes provide consistent simulations of both techniques. Below, we describe each of the newly available measurement technique capabilities in detail.

New ARTS features also cover a number of physical processes affecting electromagnetic propagation, which were neglected before. These include for example Doppler shifts due to wind and planet rotation, the Zeeman effect, Faraday rotation, and dispersion, which all are described in Section 3.3. In order to model several of these effects, additional model input characterising the atmosphere is required. Section 3.4 provides details on the handling of these input parameters.

Active measurement techniques provide more diverse measurement parameters. Therefore, the measurement module output has been extended. This also allows for more detailed output for passive measurement simulations. An overview is given in Section 3.5.

Geosci. Model Dev. Discuss., https://doi.org/10.5194/gmd-2017-229
Manuscript under review for journal Geosci. Model Dev.
Discussion started: 11 October 2017
© Author(s) 2017. CC BY 4.0 License.

3.1 Radio link budgets

A basic handling of radio link budgets has been introduced. The implementation focuses on attenuation of the power between a transmitter of a coherent signal and the receiver position, but also some other aspects are covered by the auxiliary variables provided. The latter includes a basic treatment of radio occultation, i.e. when a coherent microwave signal, such as from GNSS, is recorded by either a satellite- or ground-based receiver in order to determine certain atmospheric properties (e.g. Kursinski et al., 2000; Nilsson and Elgered, 2008). Only an overview of these additions is given here, for details see Eriksson et al. (2011c) and the built-in documentation.

The most critical step of these calculations is to establish the propagation path between transmitter and receiver. This step is so far only handled by a quite simple and time consuming algorithm (Eriksson et al., 2011c) and only considers effects covered by geometrical optics. So called multi-pathing is not treated, the algorithm settles with finding a single link path, or to determine that no path is possible due to interception by the planet's surface.

On the other hand, the receiver and transmitter can be placed at arbitrary positions, allowing that, for example, satellite-to-satellite as well as aircraft-to-ground radio links can be analysed. All atmospheric dimensionalities are handled (1D, 2D and 3D).

The dominating attenuation term is the "free space loss". This term is in ARTS defined as $1/(4\pi l^2)$, where l is the distance along the line of sight. A probably more common definition of the term is $(\lambda/(4\pi l))^2$, where λ is the wavelength, but this version is avoided as it includes the variation of the receiver's gain with frequency, while in ARTS the ambition is to keep atmospheric and sensor effects strictly apart. Attenuation due to gases and particles are included exactly in the same manner as for pure transmission calculations.

A special effect when transmitting coherent signals is (de)focusing. Simply expressed, the effect originates in the fact that refraction can vary over the wavefront. Defocusing occurs if neighbouring ray-paths in a medium diverge more quickly than for free space propagation. The opposite, focusing, can also take place, but is in general less pronounced. ARTS provides a general and rough estimate of (de)focusing by simply determining the propagation path at two slightly shifted propagation angles, starting at the transmitter, and comparing the distance between the two paths, at the receiver, to the distance expected from pure geometry. For satellite-to-satellite links, the user can instead select to make use of some standard analytical approximations (e.g. given in Kursinski et al., 2000, Sec. 3.7), where both the defocusing and focusing components are considered.

For a more complete characterisation of the radio link, the auxiliary output at hand includes the following quantities: bending angle, impact parameter (both defined as in Figure 1), extra path delay, Faraday rotation and all loss terms reported individually.

3.2 Back-scattering radars

Another active technique now partly treated is atmospheric back-scattering radar. The module for this task, developed as part of Galligani et al. (2015), handles the direct back-scattering together with atmospheric propagation and attenuation, giving full consideration of polarimetric aspects in both parts. Features not yet treated include the influence of the planet's surface, multiple scattering and Doppler shifts of the radar pulse itself. Multiple scattering refers here to the reception of photons scattered more

Geosci. Model Dev. Discuss., https://doi.org/10.5194/gmd-2017-229
Manuscript under review for journal Geosci. Model Dev.
Discussion started: 11 October 2017
© Author(s) 2017. CC BY 4.0 License.

Geoscientific Model Development Discussions

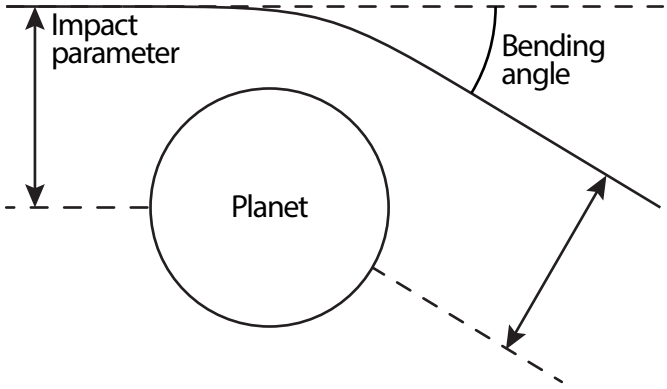

Figure 1. The radio occultation geometry with impact parameter and bending angle. See for example Kursinski et al. (2000) for details.

than once, while two-way attenuation due to particle absorption and scattering is considered. That is, when multiple scattering is significant, the simulated radar return will be an underestimation of the true value; see Battaglia et al. (2010) for a review when multiple scattering requires consideration.

Each observation of back-scattering, $\mathbf{y}$, is simulated as

$$\mathbf{y} = \mathbf{p} \cdot \mathbf{T}_h \mathbf{Z}(\Omega = 180°) \mathbf{T}_a \mathbf{s}_t, \tag{9}$$

where $\mathbf{s}_t$ is a unit vector representing the transmitted pulse (including its polarisation state), $\mathbf{T}_a$ is the transmission from the transmitter/receiver to the scattering point, $\mathbf{Z}(\Omega = 180°)$ is the value of the scattering (or phase) matrix for backward scattering, $\mathbf{T}_h$ is equivalent to $\mathbf{T}_a$ but is valid for the opposite direction, and $\mathbf{p}$ is vector describing the polarisation response of the receiver. For vector radiative transfer, the transmission can depend on direction, and $\mathbf{T}_h$ and $\mathbf{T}_a$ are not necessarily equal. The above is an extension of the traditional, scalar, radar equation (e.g. Battaglia et al., 2010, Eq. 1):

$$\beta_a(l) = \beta(l) e^{-2\tau(l)}, \tag{10}$$

where β and β_a are local and "apparent" back-scattering coefficient respectively, l is the distance to the radar, and τ is the optical depth.

The output of Equation 9 can be provided both as a function of altitude or round-trip time, in units of either back-scattering coefficient (1/(m·sr)) or radar reflectivity (Ze) (in both cases, the mean inside each altitude or time bin). Observations outside the zenith and nadir directions are allowed.

3.3 General radiative transfer features

This section presents new features in ARTS that are of radiative transfer character and of general applicability, i.e. that can be used together with the different measurement technique modules.

Geosci. Model Dev. Discuss., https://doi.org/10.5194/gmd-2017-229
Manuscript under review for journal Geosci. Model Dev.
Discussion started: 11 October 2017
© Author(s) 2017. CC BY 4.0 License.

Geoscientific Model Development Discussions

3.3.1 Handling of non-particle polarisation

Older ARTS versions have assumed that only particulate matter (including the planet's surface) causes effects that go beyond a scalar description. That is, gaseous absorption has been seen as scalar attenuation coefficients. This limitation is now removed, for two reasons. First of all, the Zeeman effect (Section 3.3.3) causes the absorption to depend on polarisation, which cannot be described in a scalar manner. Secondly, effects of magneto-optical (del Toro Iniesta, 2003, Sec. 1) character also do not fit into a scalar formalism, and both Faraday rotation and parts of the Zeeman effects fall into this category.

Accordingly, the code has been revised to throughout allow for a matrix description of propagation effects. As a consequence, the terminology used in ARTS has also changed, what was before denoted as "absorption coefficient" is now called "propagation matrix" (following e.g. del Toro Iniesta, 2003) to reflect the wider scope of the associated variables and methods. This extension made it also possible to add a feature treating particulate matter as purely absorbing matter. This allows for a much faster treatment of radiative transfer when scattering is neglected. This simplification is only valid when the particles are small compared to the wavelength, i.e. their single scattering albedo is small. There is no check in ARTS, though, that this condition is fulfilled; this judgement is fully left to the user.

3.3.2 Faraday rotation

A wave propagating through the ionosphere will force free electrons to move in curved paths. For example, if the incident wave is circularly polarised, the motion of the electrons will be circular. Consequently, the refractive index is not a single constant, but depends on polarisation. More precisely, left and right hand polarised waves will propagate with different speeds. As a plane polarised wave can be thought of as a linear superposition of a left hand and a right hand polarised wave with equal amplitudes but different phase, the plane of polarisation will then rotate as the wave is propagating through the media. This is denoted as Faraday rotation, and this physical mechanism is now handled by ARTS. The core expression is (e.g. Rybicki and Lightman, 1979)

$$r = \frac{e^3}{8\pi^2 c\epsilon_0 m^2 f^2} n_e(s)\mathbf{B}(s)\cdot\hat{\mathbf{s}}, \tag{11}$$

where r is the change in rotation angle [rad/m], e is the charge of an electron, c is the vacuum speed of light, ϵ_0 is the permittivity of vacuum, m is the electron mass, f is the frequency, $n_e(s)$ is the density of electrons at point s, $\mathbf{B}$ is the magnetic field, $\cdot$ denotes the dot (scalar) product and $\hat{\mathbf{s}}$ is the unit vector along the propagation direction. See Eriksson et al. (2011c) for further details.

3.3.3 Zeeman effect

Molecules with unpaired electrons experience an effect named the Zeeman effect after its discoverer (Zeeman, 1897). The Zeeman effect polarises the radiation as a function of magnetic field orientation, and splits what is otherwise a single spectral

Geosci. Model Dev. Discuss., https://doi.org/10.5194/gmd-2017-229
Manuscript under review for journal Geosci. Model Dev.
Discussion started: 11 October 2017
© Author(s) 2017. CC BY 4.0 License.

Geoscientific Model Development Discussions

line into several lines, with a splitting distance that is a function of the magnetic field strength. The total line strength is kept constant but distributed over the split lines.

The physical mechanism, from which the effect arises, is that the spin of the unpaired electrons couples to the external magnetic field, changing the energy state of the molecule as a function of magnetic field strength by

$$\Delta E = -gM|\mathbf{B}|\mu_b, \tag{12}$$

where g is the state-dependent Landé factor, M is the projection of the total angular momentum number J along the magnetic field, $|\mathbf{B}|$ is the magnetic field magnitude, and μ_b is the Bohr magneton. See e.g. Figures 4 and 7 in Larsson et al. (2014) for an example of how the Zeeman effect influences the brightness temperature signal as perceived by a sensor. M belongs to the set $\{-J, -J+1, \cdots, J-1, J\}$, and can only change by -1, 0, or 1 during a transition. This makes for a total of $3(2J+1)$ lines in place of the single original line.

The change in projection of J is related to the polarisation of the radiation and is influenced by the angle between the magnetic field and the path of propagation of the radiation. If the magnetic field is in the plane of observation, transitions with a changing M affect linear polarisation along the magnetic field and transitions with a constant M affect linear polarisation perpendicular to the magnetic field. If the magnetic field is pointing directly towards or away from the observer, only transitions with a changing M affect the radiation. This radiation will have its circular polarisation state altered. The implementation and the physics of the Zeeman effect in ARTS are described in detail by Larsson et al. (2014) and Larsson (2014), and references therein.

From an ARTS user perspective, the main practical requirement for Zeeman calculations is that the magnetic field must be specified as an additional input field. Some additional spectroscopic parameters are also needed. For molecular oxygen (O_2), the only tested Zeeman absorption species so far, these parameters are included with the ARTS distribution. Other species, like NO and SO, are also Zeeman-affected (see, e.g. Veseth, 1977; Christensen and Veseth, 1978), and while ARTS should be able to model the effect also for these species, this remains mostly untested at the time of writing.

The ARTS Zeeman calculations have been validated in some studies so far: Navas-Guzmán et al. (2015) simulated ground-based observations of mesospheric molecular oxygen spectra in linear polarization for several observational directions, and found good agreement with observations; Larsson et al. (2016) compared the ARTS simulations for a down-looking meteorological sensor to observations and to another, stronger parameterised Zeeman model. The module has also been applied to theoretical studies on mapping Martian surface magnetism (Larsson et al., 2013, 2017).

3.3.4 Doppler shifts

A basic treatment of Doppler shifts due to winds has existed in ARTS for some time. For ARTS 2.2 this part was completely recoded, and the Jacobian of observations with respect to the three standard wind components (u, v and w) can now also

Geosci. Model Dev. Discuss., https://doi.org/10.5194/gmd-2017-229
Manuscript under review for journal Geosci. Model Dev.
Discussion started: 11 October 2017
© Author(s) 2017. CC BY 4.0 License.

be calculated. The immediate motivation for this extension was the wind retrievals presented in Rüfenacht et al. (2014). The Doppler shift $\Delta\nu$ is given as

$$\Delta\nu = \frac{-v\nu_0 \cos(\gamma)}{c}, \tag{13}$$

where v is the wind speed, ν_0 is the rest frequency and γ is the angle between the wind direction and the line-of-sight. More details are found in Eriksson et al. (2011c). Note that the Doppler shift caused by the random thermal motion of air molecules is part of the line shape, the function describing the frequency dependence of the absorption of each transition, and is therefore not modeled explicitly here.

The rotation of the planet is another possible cause of Doppler shifts. This effect can be a concern for satellite measurements, but there is no net impact if the observer follows the planet's rotation, such as for ground-based observations of the planet's own atmosphere. In ARTS, this Doppler effect can be included by mapping the planet's rotation to a zonal wind speed, the u component. This pseudo-wind, v'_{u}, is calculated as

$$v'_{\mathrm{u}} = \frac{2\pi \cos(\alpha)(r+z)}{t_p}, \tag{14}$$

where α is the latitude, r is the local planet radius, z is the altitude and t_p is the planet's rotational period. This term is added to the true zonal wind speed.

Further, for moving observation platforms, such as aircraft or satellites, the sensor velocity can result in a significant Doppler shift and ARTS provides now a rudimentary handling of this aspect. However, the platforms are normally moving with a constant speed and the associated Doppler shift is probably most easily handled outside of the forward model.

3.3.5 Dispersion

By default, ARTS assumes that the propagation path is common for all frequencies, i.e. there is no dispersion. This is an approximation, because the atmosphere is dispersive at frequencies around strong transitions. However as discussed in Buehler et al. (2005a), this effect can safely be neglected because it is associated with very high absorption. On the other hand, the introduction of Faraday rotation, which is frequency dependent (see Equation 11), demanded to add a feature to handle dispersion. This was solved by making it possible to optionally have frequency as the outermost loop in the calculation, so that propagation paths are recalculated for each individual frequency.

This solution is completely general, so that Faraday rotation can be combined with all other features of ARTS. It also means that dispersion can now be modeled explicitly, if one is willing to pay the price of significantly increased computational cost for the calculation of the individual frequency-dependant propagation paths.

Geosci. Model Dev. Discuss., https://doi.org/10.5194/gmd-2017-229
Manuscript under review for journal Geosci. Model Dev.
Discussion started: 11 October 2017
© Author(s) 2017. CC BY 4.0 License.

3.3.6 The n^2 radiance law

ARTS has been corrected regarding passive observations, where the n^2 radiance law was not fully considered before. This law says that, even in the absence of attenuation, the radiance changes along the propagation path due to refraction effects. The preserved quantity is (Mobley, 1994; Mätzler and Melsheimer, 2006):

$$\frac{I'}{n^2} \tag{15}$$

where I' is the uncorrected radiance and n is the (real part of the) refractive index. It can be shown that it suffices to consider the refractive index at the point of emission and the point where the measurement is performed (Mobley, 1994, Eq. 4.23). To incorporate the n^2-law in the description of emission turns out to be equivalent to replacing the local propagation speed with the vacuum speed in the Planck blackbody expression. This feature was already in place, but now also a scaling with n^{-2} at the measurement position is applied in ARTS. This change affects only observations performed within the model atmosphere, as the relevant n for satellite-based observations is unity. This particular treatment of the n^2-law is discussed further in Eriksson et al. (2011b).

3.3.7 Continuum models

A number of gas absorption continuum models are available with ARTS. This particularly covers models for the micro- and millimeter-wave region (e.g. Liebe et al., 1993; Rosenkranz, 1993, 1998), but also several editions of the Clough-Kneizys-Davies continuum model (CKD, Clough et al., 1989, 2005), later enhanced by Mlawer and Tobin (MT_CKD, Mlawer et al., 2012), models that cover the entire millimeter to infrared spectral range. However, all of these continua have been developed with focus on Earth observations. In atmospheres with different major atmospheric constituents as well as pressure and temperature conditions, different continua play important roles.

Recent editions of the HITRAN database offer collision-induced absorption (CIA) data (Richard et al., 2012). CIA is caused by collisions of centro-symmetric molecules that possess no permanent electric dipole, like O_2, N_2, H_2, CO_2, and CH_4, but for which collisions create a transient dipole. The absorption strength of CIA is characterised by its dependence on the molecular density of both molecular species involved in the collision:

$$\alpha_{i,j} = \kappa_{i,j}\, n_i\, n_j, \tag{16}$$

where i and j denote the two species involved, α is the absorption coefficient, κ the binary absorption cross section, and n the number density of the respective species.

Tabulated frequency and temperature dependent $\kappa_{i,j}$ for a varity of species i and j are available from recent HITRAN editions. For the planetary toolbox with a focus on Venus, Mars and Jupiter, CIA data for CO_2-CO_2, H_2-H_2, and H_2-He are of particular interest. A mechanism to consider bi-species dependent absorption has been implemented, where tabulated binary

Geosci. Model Dev. Discuss., https://doi.org/10.5194/gmd-2017-229
Manuscript under review for journal Geosci. Model Dev.
Discussion started: 11 October 2017
© Author(s) 2017. CC BY 4.0 License.

cross sections have to be provided to ARTS. A method to derive $\kappa_{i,j}$ from HITRAN data is available. To make the HITRAN data seemlessly work with ARTS, we created a slightly modified version of the data in native ARTS format: data sets covering the same frequency range have been merged into one frequency-temperature table, data sets only covering visible and shorter wavelengths have been removed, and all binary cross sections have been converted from HITRAN ($cm^5/molec^2$) to ARTS ($m^5/molec^2$) units. These data are available as part of the arts-xml-data package.

3.4 Extended atmospheric state characterisation

Several of the new physical processes described above require additional input parameters in order to be properly modeled. Doppler shifts from wind require characterisation of the wind, Zeeman effect and Faraday rotation require magnetic field knowledge, and Faraday rotation and ionospheric refraction require a description of the electron density.

All non-scattering atmospheric matter in ARTS is subsumed as absorption species with associated atmospheric fields gathered into a variable named vmr_field. Following this approach, free electrons have been added to the list of allowed absorption species, and when considering free electrons in a radiative transfer calculation, the electron density field (m^{-3}) is held as one entry in vmr_field.

Winds as well as the magnetic field are vector parameters, hence require three pieces of information per atmospheric grid point. For both parameters, variables have been created to hold the (up to) three dimensional fields of the individual vector components u, v, and w. Generally, parameters that are not explicitly set are interpreted as equivalent to zero winds and magnetic field components, respectively.

3.5 Auxiliary output

The main output of ARTS' radiative transfer part is a vector with all simulated observations appended, i.e. directly matching the "measurement vector" $\mathbf{y}$ in the formalism of Rodgers (2000). Auxilary data that is input or output of ARTS workspace methods, such as the observational position(s) associated to a radiative transfer calculation, are always at hand. However, in many cases there exists also an interest in additional information calculated inside the radiative transfer methods. A typical example is the optical thickness related to an observational setup. Other commonly requested quantities include absorption, temperature and volume mixing ratios along the propagation path.

A general approach for obtaining such additional auxiliary data has been added to ARTS. The exact set of auxiliary variables that can be obtained differs depending on what radiative transfer problem has been solved. For example, there is no need to cover optical thickness by methods that have atmospheric transmission as main output. The auxiliary variables at hand can be divided into two main classes. The first class is the variables defined along the propagation path (such as temperature and partial transmissions). This class can just be obtained for single pencil beam calculations. This is because there is no common propagation path in the general case, considering a finite field of view, where a weighting of results from different propagation paths with the antenna pattern is performed. The second class consists of quantities resulting in a scalar value for each simulated observation value, that can be provided also for simulations including weighting with sensor characteristics. This class includes optical thickness and flags reporting intersection with the ground or the "cloud box".

Geosci. Model Dev. Discuss., https://doi.org/10.5194/gmd-2017-229
Manuscript under review for journal Geosci. Model Dev.
Discussion started: 11 October 2017
© Author(s) 2017. CC BY 4.0 License.

3.6 Remaining restrictions and outlook

Although ARTS is a fairly general radiative transfer model, several important restrictions remain. Perhaps the biggest one is that there is no collimated beam radiation source, so the model is not suitable for modelling the scattering of solar radiation in the atmosphere. Version 2.2, the subject of this article, also does not allow handling absorption and emission for conditions outside of local thermodynamic equilibrium (non-LTE). This may change in a future release, because work in this direction is ongoing.

Line mixing, a phenomenon where closely spaced molecular energy levels affect the shape of the spectral lines, is also not treated in this version. The phenomenon is important, because it affects two molecules of high scientific interest, CO_2 and O_2. For the former, line mixing is important for calculating correct energy fluxes, as needed by atmospheric circulation models and simpler radiative-convective equilibrium models. For the latter, line mixing is important for temperature remote sensing in the microwave spectral range. This aspect is in active development, and future releases of ARTS are planned to include line mixing for both species.

Other less prominent restrictions are that ARTS does not handle birefringence, handles ionospheric propagation only at frequencies well above the plasma frequency, and does propagation path calculations only by geometric optics (it is not a wave optics propagator). Also, while the model has simple surface models (specular and Lambertian) or accepts general bidirectional surface reflectivity as input, there is no explicit subsurface model, which might be of interest for complex surfaces such as snow.

4 Summary and conclusions

This article described version 2.2 of the atmospheric radiative transfer simulator ARTS. Its most significant innovation is the planetary toolbox, which allows radiative transfer simulations for other solar system planets, in addition to Earth, but should also benefit the studies of bodies beyond the solar system like exoplanets. The necessary adaptations have made the program more general in several important aspects, as described above, which benefits also applications for Earth's atmosphere. As an example, several parameters that were hardcoded before, such as isotopologue ratios, can now be read from data files, which allows easy sensitivity studies with modified parameter values.

Code and data availability. The model, together with extensive documentation, associated tools, and input data, is freely available under a GNU public license from www.radiativetransfer.org. The web page also hosts dedicated email lists for ARTS users and developers.

Competing interests. The authors declare that they have no competing interests.

Geosci. Model Dev. Discuss., https://doi.org/10.5194/gmd-2017-229
Manuscript under review for journal Geosci. Model Dev.
Discussion started: 11 October 2017
© Author(s) 2017. CC BY 4.0 License.

Acknowledgements. We would like to acknowledge the tremendous support from the ARTS developer and user community. For example, they contribute by answering questions by new users on the ARTS email lists.

We also acknowledge financial support, most importantly from the European Space Agency (ESA) in the context of contract No 4000104175/11/NL/AF "Microwave propagation toolbox for planetary atmospheres". As part of this contract, Bengt Rydberg performed work that helped to implement handling of radio links. Stefan Buehler's contribution was also supported through the Cluster of Excellence CliSAP 328 (EXC177), Universität Hamburg, funded through the German Science Foundation (DFG).

© Author(s) 2017. CC BY 4.0 License.

References

Bailey, J. and Kedziora-Chudczer, L.: Modelling the spectra of planets, brown dwarfs and stars using VSTAR, Mon. Not. R. Astron. Soc., 419, 1913–1929, https://doi.org/10.1111/j.1365-2966.2011.19845.x, 2012.

Battaglia, A., Tanelli, S., Kobayashi, S., Zrnic, D., Hogan, R. J., and Simmer, C.: Multiple-scattering in radar systems: A review, J. Quant. Spectrosc. Radiat. Transfer, 111, 917–947, 2010.

Bernstein, L. S., Berk, A., and Sundberg, R. L.: Application of MODTRAN to extra-terrestrial planetary atmospheres, Tech. rep., Spectral Sciences, Inc., Burlington, MA, technical report, 2007.

Buehler, S. A., Kuvatov, M., John, V. O., Leiterer, U., and Dier, H.: Comparison of Microwave Satellite Humidity Data and Radiosonde Profiles: A Case Study, J. Geophys. Res., 109, D13103, https://doi.org/10.1029/2004JD004605, 2004.

Buehler, S. A., Eriksson, P., Kuhn, T., von Engeln, A., and Verdes, C.: ARTS, the atmospheric radiative transfer simulator, J. Quant. Spectrosc. Radiat. Transfer, 91, 65–93, https://doi.org/10.1016/j.jqsrt.2004.05.051, 2005a.

Buehler, S. A., Verdes, C. L., Tsujimaru, S., Kleinboehl, A., Bremer, H., Sinnhuber, M., and Eriksson, P.: Expected Performance of the SMILES Submillimeter-Wave Limb Sounder compared to Aircraft Data, Radio Sci., 40, RS3016, https://doi.org/10.1029/2004RS003089, 2005b.

Buehler, S. A., Courcoux, N., and John, V. O.: Radiative transfer calculations for a passive microwave satellite sensor: Comparing a fast model and a line-by-line model, J. Geophys. Res., 111, D20304, https://doi.org/10.1029/2005JD006552, 2006a.

Buehler, S. A., von Engeln, A., Brocard, E., John, V. O., Kuhn, T., and Eriksson, P.: Recent developments in the line-by-line modeling of outgoing longwave radiation, J. Quant. Spectrosc. Radiat. Transfer, 98, 446–457, https://doi.org/10.1016/j.jqsrt.2005.11.001, 2006b.

Buehler, S. A., John, V. O., Kottayil, A., Milz, M., and Eriksson, P.: Efficient Radiative Transfer Simulations for a Broadband Infrared Radiometer — Combining a Weighted Mean of Representative Frequencies Approach with Frequency Selection by Simulated Annealing, J. Quant. Spectrosc. Radiat. Transfer, 111, 602–615, https://doi.org/10.1016/j.jqsrt.2009.10.018, 2010.

Buehler, S. A., Eriksson, P., and Lemke, O.: Absorption lookup tables in the radiative transfer model ARTS, J. Quant. Spectrosc. Radiat. Transfer, 112, 1559–1567, https://doi.org/10.1016/j.jqsrt.2011.03.008, 2011.

Cess, R. D.: A radiative transfer model for planetary atmospheres, J. Quant. Spectrosc. Radiat. Transfer, 11, 1699–1710, https://doi.org/10.1016/0022-4073(71)90148-8, 1971.

Christensen, H. and Veseth, L.: On the high-precision Zeeman effect in O_2 and SO, J. Molec. Struct., 72, 438–444, https://doi.org/10.1016/0022-2852(78)90142-X, 1978.

Clough, S. A., Kneizys, F. X., and Davies, R. W.: Line Shape and the Water Vapor Continuum, Atmos. Res., 23, 229–241, https://doi.org/10.1016/0169-8095(89)90020-3, 1989.

Clough, S. A., Shephard, M. W., Mlawer, E. J., Delamere, J. S., Iacono, M., Cady-Pereira, K., Boukabara, S., and Brown, P. D.: Atmospheric radiative transfer modeling: a summary of the AER codes, J. Quant. Spectrosc. Radiat. Transfer, 91, 233–244, https://doi.org/10.1016/j.jqsrt.2004.05.058, 2005.

Davis, C., Emde, C., and Harwood, R.: A 3D Polarized Reversed Monte Carlo Radiative Transfer Model for mm and sub-mm Passive Remote Sensing in Cloudy Atmospheres, IEEE T. Geosci. Remote, 43, 1096–1101, https://doi.org/10.1109/TGRS.2004.837505, 2005.

Davis, C. P., Evans, K. F., Buehler, S. A., Wu, D. L., and Pumphrey, H. C.: 3-D polarised simulations of space-borne passive mm/sub-mm midlatitude cirrus observations: a case study, Atmos. Chem. Phys., 7, 4149–4158, https://doi.org/10.5194/acp-7-4149-2007, 2007.

del Toro Iniesta, J. C.: Introduction to spectropolarimetry, Cambridge university press, 2003.

© Author(s) 2017. CC BY 4.0 License.

Dudhia, A.: The Reference Forward Model (RFM), J. Quant. Spectrosc. Rad. Transfer, 186, 243–253, 2017.

Emde, C., Buehler, S. A., Davis, C., Eriksson, P., Sreerekha, T. R., and Teichmann, C.: A Polarized Discrete Ordinate Scattering Model for Simulations of Limb and Nadir Longwave Measurements in 1D/3D Spherical Atmospheres, J. Geophys. Res., 109, D24207, https://doi.org/10.1029/2004JD005140, 2004a.

Emde, C., Buehler, S. A., Eriksson, P., and Sreerekha, T. R.: The effect of cirrus clouds on microwave limb radiances, Atmos. Res., 72, 383–401, https://doi.org/10.1016/j.atmosres.2004.03.023, 2004b.

Emde, C., Buras-Schnell, R., Kylling, A., Mayer, B., Gasteiger, J., Hamann, U., Kylling, J., Richter, B., Pause, C., Dowling, T., and Bugliaro, L.: The libRadtran software package for radiative transfer calculations (version 2.0.1), Geosci. Model Dev., 9, 1647–1672, https://doi.org/10.5194/gmd-9-1647-2016, 2016.

Eriksson, P., Merino, F., Murtagh, D., Baron, P., Ricaud, P., and de La Noë, J.: Studies for the Odin sub-millimetre radiometer: 1. Radiative transfer and instrument simulation, Canadian Journal of Physics, 80, 321–340, 2002.

Eriksson, P., Jiménez, C., Murtagh, D., Elgered, G., Kuhn, T., and Buehler, S.: Measurement of tropospheric/stratospheric transmission at 10–35 GHz for H_2O retrieval in low Earth orbiting satellite links, Radio Sci., 38, 8069, https://doi.org/10.1029/2002RS002638, 2003.

Eriksson, P., Jiménez, C., and Buehler, S. A.: Qpack, a general tool for instrument simulation and retrieval work, J. Quant. Spectrosc. Radiat. Transfer, 91, 47–64, https://doi.org/10.1016/j.jqsrt.2004.05.050, 2005.

Eriksson, P., Ekström, M., Melsheimer, C., and Buehler, S. A.: Efficient forward modelling by matrix representation of sensor responses, Int. J. Remote Sensing, 27, 1793–1808, https://doi.org/10.1080/01431160500447254, 2006.

Eriksson, P., Buehler, S. A., Davis, C. P., Emde, C., and Lemke, O.: ARTS, the atmospheric radiative transfer simulator, Version 2, J. Quant. Spectrosc. Radiat. Transfer, 112, 1551–1558, https://doi.org/10.1016/j.jqsrt.2011.03.001, 2011a.

Eriksson, P., Buehler, S. A., Emde, C., Sreerekha, T. R., Melsheimer, C., and Lemke, O.: ARTS-2 Theory, ARTS Development Team, regularly updated versions available at http://www.radiativetransfer.org/docs/, 2011b.

Eriksson, P., Buehler, S. A., Emde, C., Sreerekha, T. R., Melsheimer, C., and Lemke, O.: ARTS-2 User Guide, ARTS Development Team, regularly updated versions available at http://www.radiativetransfer.org/docs/, 2011c.

Eriksson, P., Rydberg, B., and Buehler, S. A.: On cloud ice induced absorption and polarisation effects in microwave limb sounding, Atmos. Meas. Tech., 4, 1305–1318, https://doi.org/10.5194/amt-4-1305-2011, 2011d.

Eshleman, V. R., Hinson, D. P., Lindal, G. F., and Tyler, G. L.: Past and future of radio occultation studies of planetary atmospheres, Adv. Space. Res., 7, 29–32, https://doi.org/10.1016/0273-1177(87)90199-2, 1987.

Fischer, J., Gamache, R. R., Goldman, A., Rothman, L. S., and Perrin, A.: Total internal partition sums for molecular species in the 2000 edition of the HITRAN database, J. Quant. Spectrosc. Radiat. Transfer, 82, 401–412, https://doi.org/10.1016/S0022-4073(03)00166-3, 2003.

Galligani, V. S., Prigent, C., Defer, E., Jimenez, C., Eriksson, P., Pinty, J.-P., and Chaboureau, J. P.: Meso-scale modelling and radiative transfer simulations of a snowfall event over France at microwaves for passive and active modes and evaluation with satellite observations, Atmos. Meas. Tech., 8, 1605–1616, https://doi.org/10.5194/amt-8-1605-2015, 2015.

Gamache, R. R., Laraia, A. L., and Lamouroux, J.: Half-widths, their temperature dependence, and line shifts for the HDO-CO_2 collision system for applications to CO_2-rich planetary atmospheres, Icarus, 213, 720–730, https://doi.org/10.1016/j.icarus.2011.03.021, 2011.

Gasteiger, J., Emde, C., Mayer, B., Buras, R., Buehler, S. A., and Lemke, O.: Representative wavelengths absorption parameterization applied to satellite channels and spectral bands, J. Quant. Spectrosc. Radiat. Transfer, 148, 99–115, https://doi.org/10.1016/j.jqsrt.2014.06.024, 2014.

© Author(s) 2017. CC BY 4.0 License.

Gordon, I. E., Rothman, L. S., Hill, C., Kochanov, R. V., Tan, Y., Bernath, P. F., Birk, M., Boudon, V., Campargue, A., Chance, K. V., Drouin, B. J., Flaud, J. M., Gamache, R. R., Hodges, J. T., Jacquemart, D., Perevalov, V. I., Perrin, A., Shine, K. P., Smith, M. A. H., Tennyson, J., Toon, G. C., Tran, H., Tyuterev, V. G., Barbe, A., Császár, A. G., Devi, V. M., Furtenbacher, T., Harrison, J. J., Hartmann, J. M., Jolly, A., Johnson, T. J., Karman, T., Kleiner, I., Kyuberis, A. A., Loos, J., Lyulin, O. M., Massie, S. T., Mikhailenko, S. N., Moazzen-Ahmadi, N., Müller, H. S. P., Naumenko, O. V., Nikitin, A. V., Polyansky, O. L., Rey, M., Rotger, M., Sharpe, S. W., Sung, K., Starikova, E., Tashkun, S. A., Vander Auwera, J., Wagner, G., Wilzewski, J., Wcisło, P., Yu, S., and Zak, E. J.: The HITRAN2016 molecular spectroscopic database, J. Quant. Spectrosc. Rad. Transfer, pp. 1–66, 2017.

Hill, C., Gordon, I. E., Rothman, L. S., and Tennyson, J.: A new relational database structure and online interface for the HITRAN database, J. Quant. Spectrosc. Radiat. Transfer, 130, 51–61, https://doi.org/10.1016/j.jqsrt.2013.04.027, 2013.

Hinson, D. P., J., F. M. F. A., Kliore, Schinder, P. J., Twicken, J. D., and Herrera, R. G.: Jupiter's ionosphere: Results from the First Galileo Radio Occultation Experiment, Geophys. Res. Lett., 24, 2107–2110, https://doi.org/10.1029/97GL01608, 1997.

Jacquinet-Husson, N., Crepeau, L., Armante, R., Boutammine, C., Chédin, A., Scott, N. A., Crevoisier, C., Capelle, V., Boone, C., Poulet-Crovisier, N., Barbe, A., Campargue, A., Chris Benner, D., Benilan, Y., Bézard, B., Boudon, V., Brown, L. R., Coudert, L. H., Coustenis, A., Dana, V., Devi, V. M., Fally, S., Fayt, A., Flaud, J.-M., Goldman, A., Herman, M., Harris, G. J., Jacquemart, D., Jolly, A., Kleiner, I., Kleinböhl, A., Kwabia-Tchana, F., Lavrentieva, N., Lacome, N., Xu, L.-H., Lyulin, O. M., Mandin, J.-Y., Maki, A., Mikhailenko, S., Miller, C. E., Mishina, T., Moazzen-Ahmadi, N., Müller, H. S. P., Nikitin, A., Orphal, J., Perevalov, V., Perrin, A., Petkie, D. T., Predoi-Cross, A., Rinsland, C. P., Remedios, J. J., Rotger, M., Smith, M. A. H., Sung, K., Tashkun, S., Tennyson, J., Toth, R. A., Vandaele, A.-C., and Vander Auwera, J.: The 2009 edition of the GEISA spectroscopic database, J. Quant. Spectrosc. Radiat. Transfer, 112, 2395–2445, https://doi.org/10.1016/j.jqsrt.2011.06.004, 2011.

John, V. O. and Buehler, S. A.: The impact of ozone lines on AMSU-B radiances, Geophys. Res. Lett., 31, L21108, https://doi.org/10.1029/2004GL021214, 2004.

John, V. O., Buehler, S. A., von Engeln, A., Eriksson, P., Kuhn, T., Brocard, E., and Koenig-Langlo, G.: Understanding the variability of clear-sky outgoing long-wave radiation based on ship-based temperature and water vapor measurements, Q. J. R. Meteorol. Soc., 132, 2675–2691, https://doi.org/10.1256/qj.05.70, 2006.

Kaplan, L. D.: Inference of Atmospheric Structure from Remote Radiation Measurements, Journal of the Optical Society of America, 49, 1004–1007, https://doi.org/10.1364/JOSA.49.001004, 1959.

Kasai, Y., Sagawa, H., Kuroda, T., Manabe, T., Ochiai, S., Kikuchi, K., Nishibori, T., Baron, P., Mendrok, J., Hartogh, P., Murtagh, D., Urban, J., von Schéele, F., and Frisk, U.: Overview of the Martian atmospheric submillimetre sounder FIRE, Planet. Space Sci., 63-64, 62–82, https://doi.org/10.1016/j.pss.2011.10.013, 2012.

Kottayil, A., Buehler, S. A., John, V. O., Miloshevich, L. M., Milz, M., and Holl, G.: On the importance of Vaisala RS92 radiosonde humidity corrections for a better agreement between measured and modeled satellite radiances, J. Atmos. Oceanic Technol., 29, 248–259, https://doi.org/10.1175/JTECH-D-11-00080.1, 2012.

Kursinski, E. R., Hajj, G. A., Leroy, S. S., and Herman, B.: The GPS radio occultation technique, Terrestrial Atmosperic Oceanic Studies, 11, 53–114, 2000.

Lammer, H., Kasting, J. F., Chasefiere, E., Johnson, R. E., Kulikov, Y. N., and Tiang, F.: Atmospheric Evolution of Terrestrial Planets and Satellites, Space Science Reviews, 139, 399–436, https://doi.org/10.1007/s11214-008-9413-5, 2008.

Laraia, A. L., Gamache, R. R., Lamouroux, J., Gordon, I. E., and Rothman, L. S.: Total internal partition sums to support planetary remote sensing, Icarus, 215, 391–400, https://doi.org/10.1016/j.icarus.2011.06.004, 2011.

© Author(s) 2017. CC BY 4.0 License.

Larsson, R.: A note on modelling of the oxygen spectral cross-section in the Atmospheric Radiative Transfer Simulator — Zeeman effect combined with line mixing in Earth's atmosphere, Int. J. Remote Sensing, 35, 4845–5853, 2014.

Larsson, R., Ramstad, R., Mendrok, J., Buehler, S. A., and Kasai, Y.: A Method for Remote Sensing of Weak Planetary Magnetic Fields: Simulated Application to Mars, Geophys. Res. Lett., 40, 5014–5018, https://doi.org/10.1002/grl.50964, 2013.

Larsson, R., Buehler, S. A., Eriksson, P., and Mendrok, J.: A treatment of the Zeeman effect using Stokes formalism and its implementation in the Atmospheric Radiative Transfer Simulator (ARTS), J. Quant. Spectrosc. Radiat. Transfer, 133, 445–453, https://doi.org/10.1016/j.jqsrt.2013.09.006, 2014.

Larsson, R., Milz, M., Rayer, P., Saunders, R., Bell, W., Booton, A., Buehler, S. A., Eriksson, P., and John, V. O.: Modeling the Zeeman effect in high-altitude SSMIS channels for numerical weather prediction profiles: comparing a fast model and a line-by-line model, Atmos. Meas. Tech., 9, 841–857, https://doi.org/10.5194/amt-9-841-2016, 2016.

Larsson, R., Milz, M., Eriksson, P., Mendrok, J., Kasai, Y., Buehler, S. A., Diéval, C., Brain, D., and Hartogh, P.: Martian magnetism with orbiting sub-millimeter sensor: simulated retrieval system, Geosci. Instr., Methods and Data Syst., 6, 27–37, https://doi.org/10.5194/gi-6-27-2017, 2017.

Le Moal, M. F. and Severin, F.: N_2 and H_2 broadening parameters in the fundamental band of CO, J. Quant. Spectrosc. Radiat. Transfer, 35, 145–152, https://doi.org/10.1016/0022-4073(86)90111-1, 1986.

Liebe, H. J., Hufford, G. A., and Cotton, M. G.: Propagation modeling of moist air and suspended water/ice particles at frequencies below 1000 GHz, in: AGARD 52nd Specialists' Meeting of the Electromagnetic Wave Propagation Panel, pp. 3–1–3–10, Palma de Mallorca, Spain, ftp://ftp.its.bldrdoc.gov/pub/mpm93/, 1993.

Manabe, S. and Möller, F.: On the radiative equilibrium and heat balance of the atmosphere, Mon. Weather Rev., 89, 503–532, https://doi.org/10.1175/1520-0493(1961)089<0503:OTREAH>2.0.CO;2, 1961.

Mathar, R. J.: Refractive index of humid air in the infrared: model fits, J. Opt. A: Pure Appl. Opt., 9, 470–476, https://doi.org/10.1088/1464-4258/9/5/008, 2007.

Mätzler, C. and Melsheimer, C.: Radiative transfer and microwave radiometry, in: Thermal microwave radiation: applications for remote sensing, edited by Mätzler, C., pp. 1–23, The institution of engineering and technology, UK, 2006.

Melsheimer, C., Verdes, C., Buehler, S. A., Emde, C., Eriksson, P., Feist, D. G., Ichizawa, S., John, V. O., Kasai, Y., Kopp, G., Koulev, N., Kuhn, T., Lemke, O., Ochiai, S., Schreier, F., Sreerekha, T. R., Suzuki, M., Takahashi, C., Tsujimaru, S., and Urban, J.: Intercomparison of General Purpose Clear Sky Atmospheric Radiative Transfer Models for the Millimeter/Submillimeter Spectral Range, Radio Sci., RS1007, https://doi.org/10.1029/2004RS003110, 2005.

Mendrok, J., Eriksson, P., and Perrin, A.: Microwave Propagation Toolbox for Planetary Atmospheres — Technical Note 3 (D5): Propagation model Technical details and expected performance, Tech. rep., ESTEC Contract No 4000104175/11/NL/AF, 2014.

Mlawer, E. J., Payne, V. H., Moncet, J.-L., Delamere, J. S., Alvarado1, M. J., and Tobin, D. C.: Development and recent evaluation of the MT_CKD model of continuum absorption, Phil. Trans. R. Soc. A, 370, 2520–2556, https://doi.org/10.1098/rsta.2011.0295, 2012.

Mobley, C. D.: Light and water: radiative transfer in natural waters, Academic Press, USA, 1994.

Navas-Guzmán, F., Kämpfer, N., Murk, A., Larsson, R., Buehler, S. A., and Eriksson, P.: Zeeman effect in atmospheric O_2 measured by ground-based microwave radiometry, Atmos. Meas. Tech., pp. 1863–1874, https://doi.org/10.5194/amt-8-1863-2015, 2015.

Newell, A. C. and Baird, R. C.: Absolute Determination of Refractive Indices of Gases at 47.7 Gigahertz, J. Appl. Phys., 36, 3751–3759, https://doi.org/10.1063/1.1713942, 1965.

© Author(s) 2017. CC BY 4.0 License.

Nilsson, T. and Elgered, G.: Long-term trends in the atmospheric water vapor content estimated from ground-based GPS data, J. Geophys. Res., 113, D19101, https://doi.org/10.1029/2008JD010110, 2008.

Oschlisniok, J., Häusler, B., Pätzold, M., Tyler, G. L., Bird, M. K., Tellmann, S., Remus, S., and Andert, T.: Microwave absorptivity by sulfuric acid in the Venus atmosphere: First results from the Venus Express Radio Science experiment VeRa, Icarus, 221, 940–948, https://doi.org/10.1016/j.icarus.2012.09.029, 2012.

Owen, T. and Encrenaz, T.: Element abundances and isotope ratios in the giant planets and Titan, Space Science Reviews, 106, 121–138, https://doi.org/10.1023/A:1024633603624, 2003.

Perrin, A., Puzzarini, C., Colmont, J.-M., Verdes, C., Wlodarczak, G., Cazzoli, G., Buehler, S., Flaud, J.-M., and Demaison, J.: Molecular line parameters for the MASTER (Millimeter wave Acquisitions for Stratosphere/Troposphere Exchange Research) database, J. Atmos. Chem., 50, 161–205, https://doi.org/10.1007/s10874-005-7185-9, 2005.

Phillips, N. A.: The general circulation of the atmosphere: A numerical experiment, Quarterly Journal of the Royal Meteorological Society, 82, 123–164, 1956.

Pickett, H., Poynter, R. L., Cohen, E. A., Delitsky, M. L., Pearson, J. C., and Müller, H. S. P.: Submillimeter, millimeter, and microwave spectral line catalog, J. Quant. Spectrosc. Radiat. Transfer, 60, 883–890, https://doi.org/10.1016/S0022-4073(98)00091-0, 1998.

Pincus, R., Mlawer, E. J., Oreopoulos, L., Ackerman, A. S., Baek, S., Brath, M., Buehler, S. A., Cady-Pereira, K. E., Cole, J. N. S., Dufresne, J.-L., Kelley, M., Li, J., Manners, J., Paynter, D. J., Roehrig, R., Sekiguchi, M., and Schwarzkopf, D. M.: Radiative flux and forcing parameterization error in aerosol-free clear skies, Geophys. Res. Lett., 42, 5485–5492, https://doi.org/10.1002/2015GL064291, 2015.

Plass, G. N.: The Influence of the 15-Mu Carbon-Dioxide Band on the Atmospheric Infra-Red Cooling Rate, Quarterly Journal of the Royal Meteorological Society, 82, 310–324, 1956.

Richard, C., Gordon, I. E., Rothman, L. S., Abel, M., Frommhold, L., Gustafsson, M., Hartmann, J.-M., Hermans, C., Lafferty, W. J., Orton, G. S., Smith, K., and Tran, H.: New section of the HITRAN database: Collision-induced absorption (CIA), J. Quant. Spectrosc. Radiat. Transfer, 113, 1276–1285, https://doi.org/10.1016/j.jqsrt.2011.11.004, 2012.

Rodgers, C.: Inverse methods for atmospheric sounding: Theory and practise, World Scientific Publishing, 1 edn., 2000.

Rosenkranz, P. W.: Absorption of microwaves by atmospheric gases, in: Atmospheric remote sensing by microwave radiometry, edited by Janssen, M. A., pp. 37–90, John Wiley and Sons, Inc., ISBN 0-471-62891-3, ftp://mesa.mit.edu/phil/lbl_rt, 1993.

Rosenkranz, P. W.: Water vapor microwave continuum absorption: A comparison of measurements and models, Radio Sci., 33, 919–928, (correction in 34, 1025, 1999), ftp://mesa.mit.edu/phil/lbl_rt, 1998.

Rothman, L. S., Gordon, I. E., Barbe, A., Benner, D. C., Bernath, P. F., Birk, M., Boudon, V., Brown, L. R., Campargue, A., Champion, J.-P., Chance, K., Coudert, L. H., Dana, V., Devi, V. M., Fally, S., Flaud, J.-M., Gamache, R. R., Goldman, A., Jacquemart, D., Kleiner, I., Lacome, N., Lafferty, W. J., Mandin, J.-Y., Massie, S. T., Mikhailenko, S. N., Miller, C. E., Moazzen-Ahmadi, N., Naumenko, O. V., Nikitin, A. V., Orphal, J., Perevalov, V. I., Perrin, A., Predoi-Cross, A., Rinsland, C. P., Rotger, M., Simeckova, M., Smith, M. A. H., Sung, K., Tashkun, S. A., Tennyson, J., Toth, R. A., Vandaele, A. C., and Auwera, J. V.: The HITRAN 2008 molecular spectroscopic database, J. Quant. Spectrosc. Radiat. Transfer, 110, 533–572, https://doi.org/10.1016/j.jqsrt.2009.02.013, 2009.

Rothman, L. S., Gordon, I. E., Babikov, Y., Barbe, A., Benner, D. C., Bernath, P. F., Birk, M., Bizzocchi, L., Boudon, V., Brown, L. R., Campargue, A., Chance, K., Cohen, E. A., Coudert, L. H., Devi, V. M., Drouin, B. J., Fayt, A., Flaud, J.-M., Gamache, R. R., Harrison, J. J., Hartmann, J.-M., Hill, C., Hodges, J. T., Jacquemart, D., Jolly, A., Lamouroux, J., Le Roy, R. J., Li, G., Long, D. A., Lyulin, O. M., Mackie, C. J., Massie, S. T., Mikhailenko, S., Müller, H. S. P., Naumenko, O. V., Nikitin, A. V., Orphal, J., Perevalov, V., Perrin, A., Polovtseva, E. R., Richard, C., Smith, M. A. H., Starikova, E., Sung, K., Tashkun, S., Tennyson, J., Toon, G. C.,

© Author(s) 2017. CC BY 4.0 License.

Tyuterev, V. G., and Wagner, G.: The HITRAN2012 molecular spectroscopic database, J. Quant. Spectrosc. Radiat. Transfer, 130, 4–50, https://doi.org/10.1016/j.jqsrt.2013.07.002, 2013.

Rüfenacht, R., Murk, A., Kämpfer, N., Eriksson, P., and Buehler, S. A.: Middle-atmospheric zonal and meridional wind profiles from polar, tropical and midlatitudes with the ground-based microwave Doppler wind radiometer WIRA, Atmos. Meas. Tech., 7, 4491–4505, https://doi.org/10.5194/amt-7-4491-2014, 2014.

Rybicki, G. B. and Lightman, A. P.: Radiative processes in astrophysics, John Wiley and Sons, Inc., USA, 1979.

Rydberg, B., Eriksson, P., and Buehler, S. A.: Prediction of cloud ice signatures in sub-mm emission spectra by means of ground-based radar and in-situ microphysical data, Q. J. R. Meteorol. Soc., 133, 151–162, https://doi.org/10.1002/qj.151, 2007.

Rydberg, B., Eriksson, P., Buehler, S. A., and Murtagh, D. P.: Non-Gaussian Bayesian retrieval of tropical upper tropospheric cloud ice and water vapour from Odin-SMR measurements, Atmos. Meas. Tech., 2, 621–637, www.atmos-meas-tech.net/2/621/2009/, 2009.

Schreier, F., Garcia, S. G., Hedelt, P., Hess, M., Mendrok, J., Vasquez, M., and Xu, J.: GARLIC - A general purpose atmospheric radiative transfer line-by-line infrared-microwave code: Implementation and evaluation, J. Quant. Spectrosc. Radiat. Transfer, 137, 29–50, https://doi.org/10.1016/j.jqsrt.2013.11.018, 2014.

Sreerekha, T. R., Buehler, S. A., O'Keeffe, U., Doherty, A., Emde, C., and John, V. O.: A strong ice cloud event as seen by a microwave satellite sensor: Simulations and Observations, J. Quant. Spectrosc. Radiat. Transfer, 109, 1705–1718, https://doi.org/10.1016/j.jqsrt.2007.12.023, 2008.

Stratton, A. J.: Optical and Radio Refraction on Venus, J. Atmos. Sci., 25, 666–667, https://doi.org/10.1175/1520-0469(1968)025<0666:OARROV>2.0.CO;2, 1968.

Thayer, G. D.: An improved equation for the radio refractive index of air, Radio Sci., 9, 803–807, 1974.

Urban, J., Dassas, K., Forget, F., and Ricaud, P.: Retrieval of vertical constituents and temperature profiles from passive submillimeter wave limb observations of the Martian atmosphere: a feasibility study, Appl. Opt., 44, 2438–2455, 2005.

Varanasi, P.: Measurement of line widths of CO of planetary interest at low temperatures, J. Quant. Spectrosc. Radiat. Transfer, 15, 191–196, https://doi.org/10.1016/0022-4073(75)90017-5, 1975.

Vasquez, M., Schreier, F., Gimeno García, S., Kitzmann, D., Patzer, B., Rauer, H., and Trautmann, T.: Infrared radiative transfer in atmospheres of Earth-like planets around F, G, K, and M stars - I. Clear-sky thermal emission spectra and weighting functions, A&A, 549, A26–1–13, https://doi.org/10.1051/0004-6361/201219898, 2013.

Verdes, C. L., Buehler, S. A., Perrin, A., Flaud, J.-M., Demaison, J., Wlodarczak, G., Colmont, J.-M., Cazzoli, G., and Puzzarini, C.: A Sensitivity Study on Spectroscopic Parameter Accuracies for a mm/sub-mm Limb Sounder Instrument, J. Molec. Spectro., 229, 266–275, https://doi.org/10.1016/j.jms.2004.09.014, 2005.

Veseth, L.: Relativistic Corrections to the Zeeman Effect in Diatomic Molecules, J. Molec. Struct., 66, 259–271, https://doi.org/10.1016/0022-2852(77)90216-8, 1977.

Zeeman, P.: On the Influence of Magnetism on the Nature of the Light Emitted by a Substance, Astrophys. J., 5, 332–347, https://doi.org/10.1086/140355, 1897.